

Keysight Technologies

KFM & CSAFM, Environmental Control in Fuel Cell Research for the Automotive Industry

Application Note



Unlocking Measurement Insights

Abstract

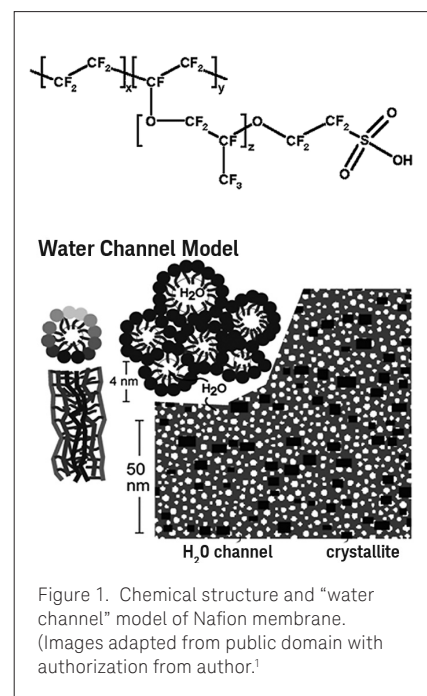
In this application note, the experimental setup for KFM and CSAFM imaging under controlled humidity using a Keysight Technologies, Inc. 5500 AFM system is illustrated. The results from the study of a proton exchange membrane using KFM and CSAFM under controlled humidity are presented. These results demonstrate that KFM and CSAFM are powerful tools for studying the surface properties and the ionic conductivity of proton exchange membranes used in fuel cell technology by the automotive industry.

Introduction

Fuel cells are among the key technologies that offer clean energy with higher conversion efficiency. Although they are already being used to power automobiles, two major challenges remain to full commercialization of fuel cell technology by the industry as well as to widespread consumer acceptance: (1) to reduce the cost so it becomes economically competitive with existing power technologies and (2) to increase the durability and lifetime of the fuel cell systems. Consequently, researchers have been focusing their efforts on developing and characterizing materials that could help in meeting these requirements.

A solid-membrane fuel cell is the most promising system for light-duty transportation and portable electronic devices. In this system, a proton exchange membrane (PEM), also known as a polymer electrolyte membrane, is sandwiched between two electrodes. The PEM allows only H^+ to pass through to complete the circuit for current flow. Therefore, the mechanical and thermal properties as well as the ionic conductivity of the PEM all play a vital role in the performance of the fuel cell. A PEM widely used in solid-membrane fuel cells is Nafion, a perfluorinated polymer that combines a hydrophobic Teflon-like backbone with hydrophilic ionic side groups. Although the structure of Nafion has drawn attention from many researchers, a detailed picture is difficult to obtain because it changes with the ratio of the two components. A recent model based on small-angle x-ray scattering experiments suggests that the Nafion membrane consists of “water channels” formed by the hydrophilic sulfonic groups supported by the hydrophobic polymer backbones and Nafion crystallites.² The chemical structure of the Nafion membrane and the “water channel” model are illustrated in Figure 1. The “water channels” provide passes for small cations like protons, while stopping anions and electrons. The diameter of these water channels depends on the water content in the membrane, averaging about 2–3 nm at 20% RH and increasing with the equilibrated relative humidity. As a result, the ionic conductivity of Nafion depends on the hydration level of the membrane, and the control of proper hydration of the PEM in a fuel cell has become a challenge in engineering design. Thus, it is critically important to understand the dependence of the ionic transport property of a PEM on its hydration state.

The solid-membrane fuel cell is a highly promising system for light-duty transportation.^{3,4} As the theoretical model suggests,² the Nafion surface consists of hydrophobic regions (corresponding to the polymer backbone) and hydrophilic regions (corresponding to the self-organized ionic side groups). Identifying these different groups on a PEM surface is a difficult task. Attempts have been made to distinguish the hydrophobic sites from the hydrophilic sites via phase imaging using AC mode AFM.³



However, the phase signal in AC mode AFM depends on the overall interaction force between the AFM tip and the sample surface, so identification of ionic clusters based on the phase image could be ambiguous in some cases. On the other hand, because the ionic clusters can exhibit different amounts of charge compared to the hydrophobic polymer region, scanning Kelvin force microscopy (KFM) can be used to directly measure the surface potential variation on the Nafion membrane. As a result, the distribution of the ionic clusters on the membrane surface can be identified from the KFM image.

Among the various experimental techniques of scanning probe microscopy, current-sensing AFM (CSAFM), also known as conducting AFM, is particularly useful for studying the transport process of protons in proton exchange membranes.⁴ In CSAFM, a Pt-coated conducting tip is utilized. In an experimental setup such as that illustrated in Figure 2, the Pt-coated AFM tip serves as the top electrode. The PEM under study is sandwiched between the AFM tip and the bottom supporting electrode, forming a localized miniature fuel cell. When a positive bias is applied to the AFM tip, $\text{H}_2\text{O} \longrightarrow \frac{1}{2} \text{O}_2 + 2\text{H}^+ + 2\text{e}^-$. The protons will then pass the PEM through existing “water channels” and recombine with electrons at the bottom electrode: $2\text{H}^+ + 2\text{e}^- \longrightarrow \text{H}_2$. Therefore, by measuring the current flowing through the AFM tip while scanning over the PEM surface at constant force, the local distribution of “active” conduction channels and the dependence of ionic conductivity on hydration level can be obtained quantitatively.

In this application note, the experimental setup for KFM and CSAFM imaging under controlled humidity using a Keysight 5500 AFM system is illustrated. The results obtained on Nafion membranes used in commercial fuel cells are presented. These results also demonstrate that KFM and CSAFM are powerful tools for fuel cell research in the automotive industry, capable of providing in situ and dynamic information about the materials in use and the catalysis and transport process of interest.

Methods and Instrumentation

Sample Preparation

Nafion 115 and Nafion 212 (purchased from CleanFuelCell, Inc.) are used for the experiments. These membranes are hot-pressed onto a Pt/C electrode. The Pt/C electrode is made of Pt films deposited on carbon cloth. A small, square piece of the membrane/electrode sample is attached to a metal substrate by gluing the corners with conductive silver paint, leaving enough space at the center for airflow. The Pt/C electrode is then

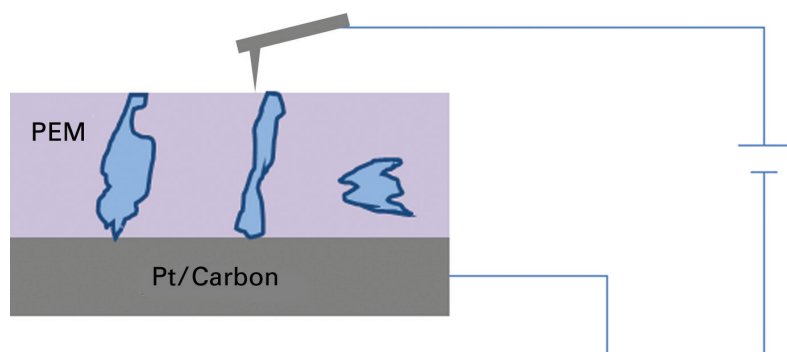


Figure 2. CSAFM study of ion conductivity of PEM. The Pt tip/PEM/Pt/Z configuration forms a miniature fuel cell in this set-up.

electrically connected to the microscope for KFM or CSAFM imaging.

Humidity Control

A Keysight 5500 AFM equipped with a PicoAPEX environmental chamber, a MAC Mode III controller, and a 90 μm multipurpose scanner is used here. The PicoAPEX chamber provides a localized environment for the sample without affecting the operation of the scanner and the controlling electronics. Experiments are carried out at 24°C with a controlled relative humidity level. Humidity control is realized by putting a beaker with water in the PicoAPEX chamber and purging dry air through the chamber. By controlling the rate of the dry airflow, a constant humidity level is maintained during the experiment.

KFM Measurement

In these experiments, KFM measurement is done via a single-pass approach with a MAC Mode III controller, which has three built-in, independent lock-in amplifiers. During KFM measurement, two lock-in amplifiers from the MAC Mode III controller are usually used simultaneously, with the first lock-in amplifier tracking the mechanical oscillation of the cantilever for topography imaging and the second lock-in amplifier tracking the electric modulation for electrostatic force measurement. The tips used for KFM measurement are Pt/Ti-coated Si tips (NSC-14 from MikroMash) with a force constant of $\sim 5 \text{ N/m}$.

The principle of KFM measurement and a detailed experimental procedure can be found in another Keysight application note.⁵ When a conductive tip is biased at a dc voltage U_{dc} against the sample surface, and a small ac modulation $U_{ac}\sin(\omega t)$ is applied to the tip simultaneously, then the total electrostatic force experienced by the tip can be expanded into a series of contributions corresponding to the basic and higher harmonics of the electric modulation

$$F_{elec} = F_{dc} + F(\omega) + F(2\omega) + \dots \quad (1)$$

The first term, F_{dc} , in Equation 1 is a dc component and does not make a contribution to surface potential measurement. The second term, $F(\omega)$, corresponding to the fundamental frequency response to the electric modulation, is given by

$$F(\omega) = -\frac{\partial C}{\partial z}(\varphi - U_{dc})\sin(\omega t) \quad (2)$$

where $\varphi = (\Phi_{sample} - \Phi_{tip})/q$ is the contact potential difference (CPD) between the sample and the tip, which is defined as the difference between the work functions, Φ_{sample} and Φ_{tip} , divided by q , the elementary charge. From Equation 2, $F(\omega) = 0$ when $U_{dc} = \varphi$ (i.e., the electrostatic force is nullified when the applied dc potential at the tip equals the CPD). Since Φ_{tip} is generally constant for a known metallic material used for the conductive tip, the variation of Φ_{sample} over the sample surface can be measured by measuring the CPD. As a result, the CPD measured from a KFM experiment is often called the surface potential of the sample. In practice, the surface potential is measured by nullifying the electrostatic force component, $F(\omega)$, with a servo-loop that supplies a dc offset to the tip.

The third term, $F(2\omega)$, in Equation 1, corresponding to the second harmonic response to the electric modulation, is given by

$$F(2\omega) = +\frac{1}{4}\frac{\partial C}{\partial z}U_{ac}^2\cos(2\omega) \quad (3)$$

Therefore, the amplitude of the second harmonic response measures dC/dz , the capacitance change at a certain height above the sample surface. As in a simple capacitor, the capacitance between two metallic electrodes depends on the dielectric properties of the

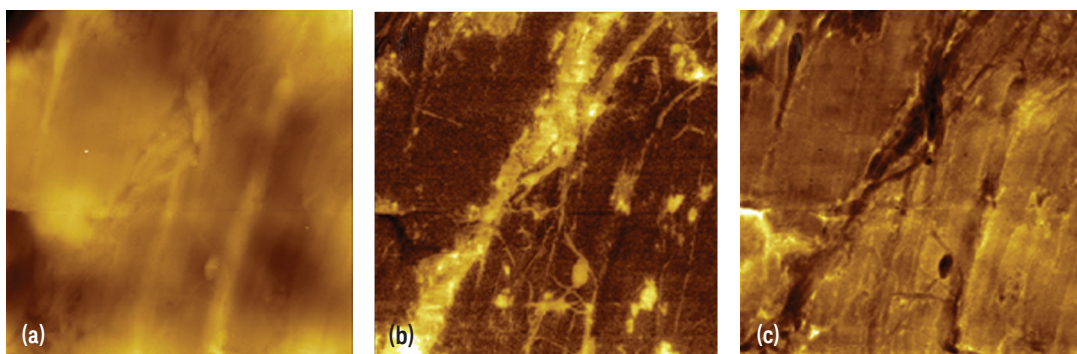


Figure 3. Topography (a), surface potential (b), and capacitance (c) images of Nafion 212 at 16% RH.

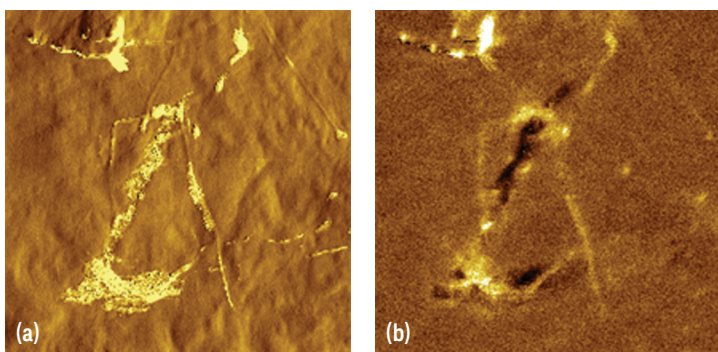


Figure 4. Phase (a) and surface potential (b) images of Nafion 115 at 37% RH.

medium materials. Consequently, the measured dC/dz provides information about the variation of dielectric and polarization properties across the sample surface.

The topography and surface potential images of Nafion 212 obtained at 16% RH are shown in Figure 3(a) and 3(b), respectively. The topography image shows that the surface of the Nafion 212 membrane has cluster-like as well as fiber-like materials spread over the surface. The surface potential image reveals that great potential difference, as high as ~ 300 mV, exists between the distinctive areas on the Nafion surface. The areas of higher surface potential correspond to the cluster- and fiber-like structures with a more positive charge density compared to the areas of lower surface potential. It is possible that the high-potential areas are associated with the hydrophobic areas and the low-potential areas are associated with the hydrophilic ionic regions. Due to screening by water molecules on the surface, the hydrophilic ionic regions show one uniform potential with less details of the underlying structure. The capacitance (dC/dz) image obtained together with the surface potential image is shown in Figure 3(c). In general, the dC/dz image shows higher amplitude for the low-potential region and lower amplitude for the high-potential region.

The effect of water on surface potential is evident when the humidity level is increased. As shown in Figure 4, at 37% RH, the surface potential image of Nafion 115 becomes largely uniform except for some particular locations. Also shown in Figure 4 is the phase image of the Nafion 115 surface collected at the same time. The phase image reveals features at the same locations on the surface as the surface potential image. However, the phase image shows constant higher phase signal for the structures, while the surface potential image gives opposite contrast for different locations over the structures. Thus, using only the phase signal to determine ionic regions on the surface could be insuf

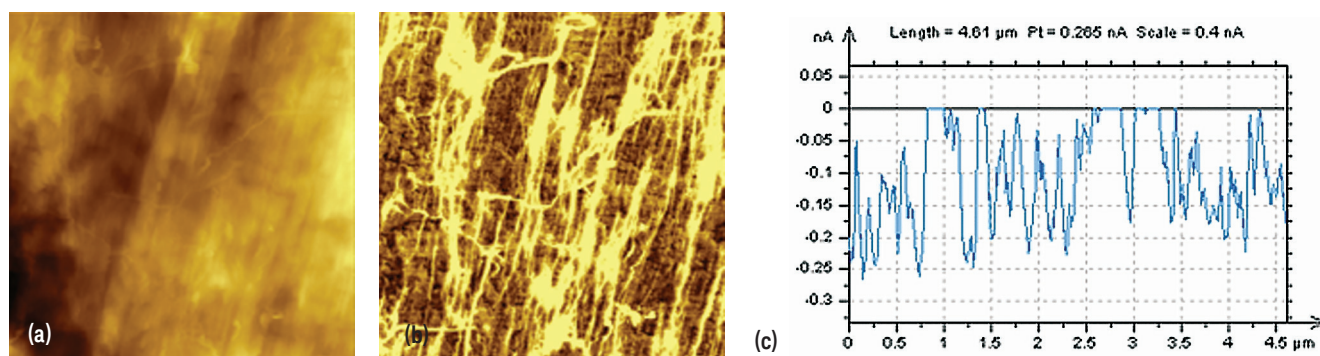


Figure 5. Topography (a), current (b), and current profile (c) for Nafion 212 at 50% RH.

ficient.

CSAFM Measurement

In these experiments, CSAFM measurement is performed using a CSAFM nose cone with a 1nA/V preamplifier that measures the current flowing through the AFM. The conductive tips are Pt/Ti-coated Si probes (CSC-17 from MikroMash) with a nominal spring constant of 0.15 N/m and a bulk resistivity of $0.01 - 0.05 \Omega \cdot \text{cm}$. Before each measurement is taken, the Nafion sample and tip are allowed to settle in the PicoAPEX chamber for 2 – 3 hours to let the humidity level stabilize.

As illustrated in Figure 2, the Pt tip/PEM/Pt/C configuration in a CSAFM measurement setup essentially forms a miniature fuel cell and the ionic transport behavior of the proton exchange membrane can be studied by measuring the conducting current through the AFM tip. The topography and current image for Nafion 212 at 50% RH is shown in Figure 5. The current profile of a single line along the horizontal direction is also presented in Figure 5. Close examination of the topography image and the current image reveals little correlation between the measured current and the topography. This indicates that the current measured is indeed associated with the ion-conductive channels existing in the membrane.

Like the surface potential image in Figure 3(b), the current image in Figure 5(b) also reveals cluster- and fiber-like structures on the surface that have a lower conductivity compared to the rest of the surface. The lower conductivity of these fiber-like structures suggests that they correspond to the hydrophobic polymer region that forms the backbone of the Nafion membrane. This conclusion is also consistent with the surface potential measurement.

However, unlike the potential measurement that measures the ionic site on the surface, the CSAFM measurement detects a conductive ionic current only when the tip is in contact with an ion transport channel that runs through the membrane (i.e., CSAFM measures only the “active channel” in the membrane). Because the ion conductivity measured with CSAFM depends on the contact area between the tip and the surface, it is important to maintain constant force during imaging. Since the tip used in this experiment is about 20 – 30 nm in size and also because of the possible existence of water meniscus at the tip-membrane interface, it is impossible to unambiguously identify individual ion channels (each of which is several nanometers in size based on the “water channel” model discussed earlier). Even though the CSAFM measurement is unable to resolve individual ion channels, it nonetheless offers a reliable method for statistically analyzing the distribution of the active ionic clusters on a membrane surface and their connection

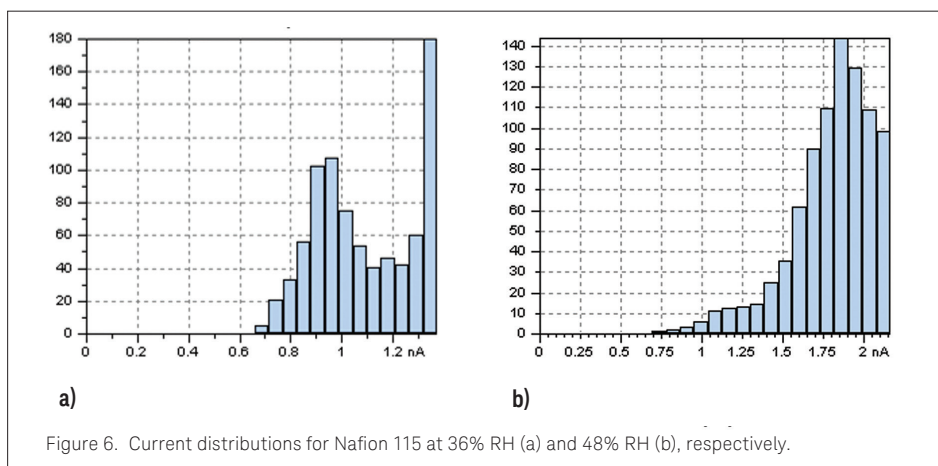


Figure 6. Current distributions for Nafion 115 at 36% RH (a) and 48% RH (b), respectively.

with the random ionic network.⁴ From the distribution, the density of proton channels and the conductance of single channels can be derived.

Figure 6 shows the current distribution for Nafion 115 at 36% RH and at 48% RH. The change in current distribution with increasing humidity suggests that as the humidity increases, formation of new active ionic clusters and expansion of the existing active ionic channels may occur. The increase in cluster size and the formation of new clusters significantly increases the interconnection between clusters, and thus conductivity.

Summary

Nafion membranes used for fuel cell manufacturing by the automotive industry are studied using KFM and CSAFM under controlled humidity. KFM images show the existence of hydrophilic and hydrophobic regions on the membrane surface, corresponding to the ionic clusters and the polymer backbones. CSAFM measurement provides reliable analysis regarding the distribution of active ionic channels in the membrane, as well as the change of ion conductivity as a function of relative humidity.

References

1. http://en.wikipedia.org/wiki/File:Nafion_structure.png
2. K. Schmidt-Rohr, Q. Chen, "Parallel cylindrical water nanochannels in Nafion fuel-cell membranes", *Nature Materials* 7 (2008) 75–83.
3. P.J. James, J.A. Elliott, T.J. McMaster, H.H. Wills, J.M. Newton, A.M.S. Elliotts, S. Hannaz, M.J. Miles, "Hydration of Nafion studied by AFM and X-ray scattering", *Journal of Materials Science* 35 (2000) 5111 – 5119.
4. X. Xie, O. Kwon, D.-M. Zhu, T. Van Nguyen, G. Lin, "Local Probe and Conduction Distribution of Proton Exchange Membranes", *J. Phys. Chem. B* 2007, 111, 6134–6140.
5. S. Magonov, J. Alexander, "Advanced Atomic Force Microscopy: Exploring Measurements of Local Electric Properties", Application Note, Keysight Technologies, Inc. (2008).

AFM Instrumentation from Keysight Technologies

Keysight Technologies offers high-precision, modular AFM solutions for research, industry, and education. Exceptional worldwide support is provided by experienced application scientists and technical service personnel. Keysight's leading-edge R&D laboratories are dedicated to the timely introduction and optimization of innovative and easy-to-use AFM technologies.

www.keysight.com/find/AFM

For more information on Keysight Technologies' products, applications or services, please contact your local Keysight office. The complete list is available at: www.keysight.com/find/contactus

Americas

Canada	(877) 894 4414
Brazil	55 11 3351 7010
Mexico	001 800 254 2440
United States	(800) 829 4444

Asia Pacific

Australia	1 800 629 485
China	800 810 0189
Hong Kong	800 938 693
India	1 800 11 2626
Japan	0120 (421) 345
Korea	080 769 0800
Malaysia	1 800 888 848
Singapore	1 800 375 8100
Taiwan	0800 047 866
Other AP Countries	(65) 6375 8100

Europe & Middle East

Austria	0800 001122
Belgium	0800 58580
Finland	0800 523252
France	0805 980333
Germany	0800 6270999
Ireland	1800 832700
Israel	1 809 343051
Italy	800 599100
Luxembourg	+32 800 58580
Netherlands	0800 0233200
Russia	8800 5009286
Spain	800 000154
Sweden	0200 882255
Switzerland	0800 805353
	Opt. 1 (DE)
	Opt. 2 (FR)
	Opt. 3 (IT)
United Kingdom	0800 0260637

For other unlisted countries:

www.keysight.com/find/contactus
(BP-10-3-16)

This information is subject to change without notice.
© Keysight Technologies, 2012 – 2017
Published in USA, February 21, 2017
5992-2182EN
www.keysight.com